European Polymer Journal 46 (2010) 977–983

Contents lists available at ScienceDirect

European Polymer Journal

journal homepage: www.elsevier.com/locate/europolj

Macromolecular Nanotechnology

Conducting poly(3,4-ethylenedioxythiophene)-montmorillonite exfoliated nanocomposites

David Aradilla [a,b], Francesc Estrany [b,c], Denise S. Azambuja [d,*], María T. Casas [a], Jordi Puiggali [a,b], Carlos A. Ferreira [e], Carlos Alemán [a,b,*]

[a] Departament d'Enginyeria Química, E.T.S. d'Enginyers Industrials, Universitat Politècnica de Catalunya, Diagonal 647, 08028 Barcelona, Spain
[b] Center for Research in Nano-Engineering, Universitat Politècnica de Catalunya, Campus Sud, Edifici C', C/Pasqual i Vila s/n, Barcelona E-08028, Spain
[c] Unitat de Química Industrial, Escola Universitària d'Enginyeria Tècnica Industrial de Barcelona, Universitat Politècnica de Catalunya, Comte d'Urgell 187, 08036 Barcelona, Spain
[d] Institute of Chemistry, Federal University of Rio Grande do Sul, Av. Bento Gonçalves 9500, CEP 91501-970 Porto Alegre, RS, Brazil
[e] Universidade Federal do Rio Grande do Sul, DEMAT, Av. Bento Gonçalves 9500, Setor 4, Prédio 74, CEP 91501-970, Porto Alegre, RS, Brazil

ARTICLE INFO

Article history:
Received 8 October 2009
Received in revised form 7 January 2010
Accepted 9 January 2010
Available online 15 January 2010

Keywords:
Poly(3,4-ethylendioxythiophene)
Montmorillonite
Nanocomposite
Conducting polymer
Nanoclay

ABSTRACT

Exfoliated nanocomposites formed by poly(3,4-ethylenedioxythiophene) and different concentrations of non-modified montmorillonite (bentonite), which range from 1% to 10% w/w, have been prepared by anodic electropolymerization in aqueous solution. Analyses of the electrochemical and electrical properties reveal that the electroactivity of the nanocomposites is higher than that of the individual homopolymer, while the electrical conductivity of the two systems is practically identical. On the other hand, the exfoliated distribution of the clay in the polymeric matrix and the morphology of the prepared materials have been characterized using transmission electron microscopy, X-ray diffraction and atomic force microscopy. The overall of the results represents a significant improvement with respect to other nanocomposites constituted by conducting polymers and clays, including those involving poly(3,4-ethylenedioxythiophene), and evidences the reliability of the preparation procedure employed in this work.

1. Introduction

The development of polymer–clay nanocomposites is a field of increasing interest due to the important technological applications of these materials. Thus, composite systems formed by organic polymers and clay minerals structured at the nanoscale level, which usually present a unique layered structure, rich intercalation chemistry and availability at low cost, have been used to develop plastic materials with advanced mechanical properties, molecular barrier behavior, fire retardant abilities, enhanced thermal stability, etc., compared to the individual polymeric materials [1–7].

On the other hand, electrically conducting polymers have also attracted much attention due to their many promising technological applications, as for example microelectronic devices, electroluminescence devices, corrosion inhibitors, electrochemomechanical devices and chemical sensors [8]. Among conducting polymers, polyaniline (PAni) and polypyrrole (PPy) are particularly attractive because of their simple synthesis, high conductivity and excellent environment stability. As a consequence, many PAni–clay [4,9–15] and PPy–clay [4,15–20] nanocomposites have been prepared and analyzed in the last years. The main effect induced by the incorporation of the clay was the improvement of the thermal stability, which was found to be higher for the nanocomposites than for the conducting polymers. Poly(3,4-ethylenedioxythiophene) (PEDOT), a polythiophene derivative with high electrical conductivity, transparency, structural stability,

* Corresponding authors.
E-mail addresses: denise@iq.ufrgs.br (D.S. Azambuja), carlos.aleman@upc.edu (C. Alemán).

0014-3057/$ - see front matter © 2010 Elsevier Ltd. All rights reserved.
doi:10.1016/j.eurpolymj.2010.01.003

suitable morphology and fast doping–undoping mechanism [21,22], has also attracted much attention. This material, which was originally described and is currently commercialized by the Bayer company, exhibits higher thermal and environmental stabilities, and easier processability than common conducting polymers, including PAni and PPy [8,21,22]. Consequently, it has been proposed for several technological applications, e.g. as sensor for specific DNA nucleotidic sequences [23], molecular condenser [24,25] and anticorrosive additive of conventional organic coatings [26].

Some hybrid nanocomposites formed by the combination of PEDOT and various inorganic materials have been reported in the last years, e.g. PEDOT–V_2O_5 [27], PEDOT–MoO_3 [28], PEDOT–graphite oxide [29] and PEDOT–clay [30,31]. PEDOT–clay nanocomposites were based on montmorillonite (MMT), a smectite group mineral clay that belongs to the general family of 2:1 layered silicates [32]. Unfortunately, PEDOT–MMT nanocomposites usually show an intercalative structure [30], which is also frequently found in PAni–MMT [32–35] and PPy–MMT [19,36–38], rather than the more desirable exfoliated organization. Thus, complete exfoliation of MMT layers in conducting polymers is a challenging task that, sometimes, requires complex and expensive strategies, e.g. modifications of MMT with intercalative agents [39] and pre-synthesis of a graft copolymer [40]. In a very recent study, an exfoliated PEDOT–MMT nanocomposite was obtained by *in situ* polymerization in an aqueous suspension containing a MMT organically modified with octadecylammonium [41]. Unfortunately, the investigations devoted to fabricate conducting polymer–clay nanocomposites using simple anodic electropolymerization methods, which are frequently used for the preparation of individual conducting polymers, are very scarce [42,43] and completely inexistent for PEDOT-containing systems. Moreover, in spite of the excellent electrochemical and electrical properties of PEDOT [21,22,44], such properties were never examined in its clay-containing nanocomposites.

In this work, we report the preparation of exfoliated PEDOT–MMT nanocomposites by electropolymerization in aqueous solution. Furthermore, the physical, electrochemical and electrical properties of the fabricated nanocomposites have been determined and compared with those obtained for PEDOT homopolymer prepared using identical experimental conditions. The paper is organized as follows. The Methods and experimental procedures are reported in the next section. After this, the preparation and electrochemical characteristics of PEDOT–MMT and PEDOT are discussed. Next, the structural, electrical and morphological characteristics of the prepared materials are examined and compared. Finally, the last section summarizes the conclusions of the work.

2. Methods

2.1. Materials

3,4-Ethylenedioxythiophene (EDOT) monomer and MMT (bentonite) were purchased from Aldrich and used as received. $LiClO_4$ analytical reagent grade from Aldrich was stored in an oven at 80 °C before use in the electrochemical trials.

2.2. Preparation

Both PEDOT and PEDOT–MMT nanocomposites were prepared by chronoamperometry (CA) under a constant potential of 1.10 V. Electrochemical experiments were performed on an Ecochimie model VersaStat II potenciostat-galvanostat using a three-electrode two-compartment cell under nitrogen atmosphere (99.995% in purity) at 25 °C. The anodic compartment was filled with 40 mL of a 10 mM monomer solution in distilled water containing 0.1 M $LiClO_4$ as supporting electrolyte, while the cathodic compartment contained 10 mL of the same electrolyte solution without the monomer. Steel AISI 316 sheets of 4 cm^2 area were employed as working and counter electrodes. The reference electrode was an Ag|AgCl electrode containing a KCl saturated aqueous solution (E° = 0.222 V vs. standard hydrogen electrode at 25 °C), which was connected to the working compartment through a salt bridge containing the electrolyte solution. All the potentials (E) given in this work refer to this electrode.

The amount of MMT in the monomer solution used to prepare PEDOT–MMT nanocomposites ranged from 1% to 10% w/w (dry weight), these concentration values being referred to that of the EDOT monomer. As a typical procedure, MMT was exfoliated in de-ionized water at neutral pH, being sonicated for 10 min with an ultrasonic generator. The resulting solution was stirred for 1 day using a magnetic stirrer. After this, a 10 mM EDOT solution in distilled water with 0.1 M $LiClO_4$ was added to the above exfoliated clay solution, and stirred for 20 h in a frozen environment (ice).

2.3. Electrochemical characterization

The electroactivity, which indicates the ability to store charge, and electrostability, which reflects the variation of the electroactivity upon successive oxidation and reduction cycles, of both the PEDOT homopolymer and the PEDOT–MMT nanocomposite were determined by cyclic voltammetry (CV). According to this procedure, electroactivity increases with the similarity between the anodic and cathodic areas of the first control voltammogram, while electrostability decreases with the oxidation and reduction areas of successive control voltammograms. A scan rate of 100 mV s^{-1} was used in all cases.

The thickness of the films (ℓ) was estimated according to Schirmeisen and Beck [45] using the mass of polymer deposited in the electrode, m_{pol}, which was obtained using the following relation:

$$m_{pol} = Q_{pol}\left(\frac{m}{Q}\right)$$

where Q_{pol} is the polymerization charge (in millicoulombs per square centimeter) consumed in the generation of each layer and $(\frac{m}{Q})$ the current productivity, the latter being previously determined for PEDOT [27] (0.875 mg C^{-1}).

Although the latter value was obtained in acetonitrile, we studied the kinetics for the oxidation–polymerization of EDOT in aqueous solution to check that it can be rightly applied in the current work. The volume of polymer deposited in the electrode (V_{pol}) was obtained using the values of m_{pol} and the density previously reported for PEDOT (1.665 g·cm^{-3}) [44]. Accordingly, the thickness of each layer was calculated considering the surface of polymerization (S_{pol}), which is the surface of the electrode (4 cm^2), and V_{pol}.

2.4. Structural, morphological and electrical characterization

The structure and distribution of the clay in the PEDOT–MMT nanocomposites were examined using a Phillips TECNAI 10 transmission electron microscope at an accelerating voltage of 100 kV. For this purpose, small strips of nanocomposite were removed from the electrode with a razor blade and, according to the manufacturer protocol, embedded in a low viscosity modified Spurr epoxy resin and curing at 60 °C for 24 h. Ultra-thin sections (less than 100 nm) of these samples were cut at room temperature using a Sorvall Porter–Blum microtome. Finally, the sections were placed on carbon coated cooper grids. Bright field micrographs were taken with an SIS Mega View II digital camera.

X-ray diffraction (XRD) spectra of PEDOT–MMT films were recorded using a Bruker D8 Advance model to 40 kV and 40 mA (λ = 1.5406 Å). The XRD patterns were taken at ambient laboratory temperature using 10 s/angular step (1 angular step = 0.02°).

Topographic AFM images were obtained with a Molecular Imaging PicoSPM using a NanoScope IV controller in ambient conditions. The averaged RMS roughness (r) was determined using the statistical application of the Nanoscope software, which calculates the average considering all the values recorded in the topographic image with exception of the maximum and the minimum. Nanometric measurements were conducted under ambient conditions at ~50% relative humidity and 20–22 °C. The system was placed on an active vibration isolation table for minimum acoustic disturbance (20 series, TMC, Peabody, MA, USA).

The electrical conductivities (σ_0) were determined using the sheet-resistance method following a previously described procedure [46].

3. Results and discussion

3.1. Preparation and electrochemical characterization

Fig. 1 (solid curve) shows the cyclic voltammogram recorded for the anodic oxidation of EDOT in distilled water with 0.1 M $LiClO_4$. Two anodic peaks, O_1 and O_2, were detected. The anodic potential of the first peak, E_p^a (O_1) = 1.38 V, is lower than that previously obtained under identical experimental conditions with exception of the acetonitrile solvent [E_p^a] (O_1) = 1.53 V] [44], while the anodic potential of the second peak O_2 overlaps the oxidation of the medium at a potential higher than 1.60 V. No reduction peak is seen in Fig. 1 because the oxidation of EDOT is an irreversible process up to 1.60 V. Uniform, adherent and insoluble PEDOT films grew on the working steel anode

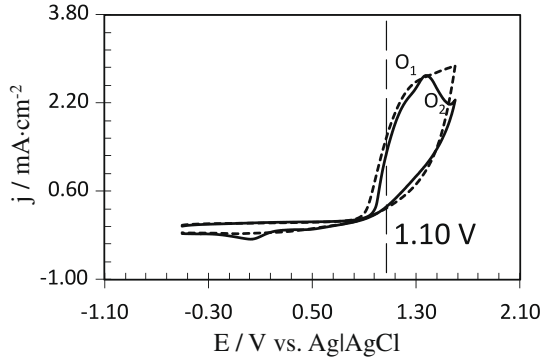

Fig. 1. Control voltammograms for the oxidation of a 10 mM of 3,4-ethylenedioxythiophene (EDOT) solution in distilled water with 0.1 M $LiClO_4$. Solid and dashed curves correspond to solutions without MMT and with 5% w/w of MMT, respectively. Voltammograms were recorded using a 4 cm^2 steel electrode. Initial and final potentials: −0.50 V; reversal potential: 1.60 V. Scan rate: 100 mV s^{-1}.

when the monomer began to be oxidized from potentials higher than 0.90 V.

The cyclic voltammograms of EDOT were used to determine the proper conditions of polymerization in an aqueous solution using $LiClO_4$ as electrolyte. Potentials comprised between 0.90 V and 1.30 V are suitable for this purpose because the anodic current densities determined from the chronoamperograms recorded at these potentials are relatively high (data not shown), i.e. the molecular diffusion of the monomer is high within this potential range. A potential of 1.10 V, which is just in the middle of such range, was chosen to generate both the PEDOT–MMT nanocomposites and PEDOT homopolymer in this work. Fig. 1 (dashed curve) presents the cyclic voltammogram recorded for the EDOT–MMT (5% w/w) solution using the same experimental conditions. As can be seen, 1.10 V is an optimal potential also in this case.

The electrogeneration of PEDOT–MMT and PEDOT films was carried out at a fixed potential of 1.10 V using a polymerization time of 300 s. The resulting films were uniform, adherent, insoluble and homogeneous in all cases. Fig. 2 compares the chronoamperograms obtained for the

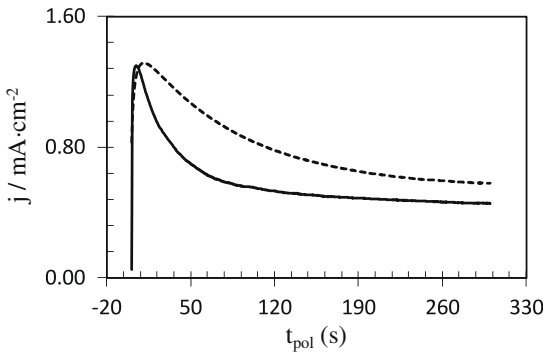

Fig. 2. Chronoamperograms recorded for the oxidation of a 10 mM of 3,4-ethylendioxythiophene (EDOT) solution in distilled water with 0.1 M $LiClO_4$ on a steel electrode by applying a constant potential of 1.10 V for a polymerization time of 300 s. Solid and dashed curves correspond to solutions without MMT and with 5% w/w of MMT, respectively.

oxidation of a 10 mM EDOT aqueous solution without and with 5% w/w MMT (solid and dashed curves, respectively). The current density stabilizes at 0.43 and 0.57 mA·cm^{-2} for PEDOT homopolymer and PEDOT–MMT (5% w/w) nanocomposite, respectively, indicating that the flow of monomer during the electrogeneration process increases upon the addition of MMT. These values clearly reflect the favourable interaction between the clay and the conducting polymer. On the other hand, it is worth noting that these values are smaller than that previously reported for PEDOT homopolymer using a constant potential of 1.40 V and acetonitrile as solvent (1.82 mA·cm^{-2}) [44], i.e. the monomer concentration and the electrolyte were identical to those employed in the current work. Thus, the effect of the polymerization conditions on the diffusion of the monomer seems to be higher than the addition of the exfoliated clay to the monomer solution.

Fig. 3 compares the control voltammograms of PEDOT and PEDOT–MMT (5% w/w) recorded in the potential range from −0.50 to 1.60 V. As can be seen, the electroactivity of the nanocomposite is higher than that of the homopolymer indicating that the addition of clay enhances the ability to store charge of PEDOT. Similarly, the electroactivity of PEDOT–MMT (1% w/w) and PEDOT–MMT (10% w/w) are higher than that of PEDOT, the difference between the nanocomposite and the homopolymer increasing with the concentration of clay (data not shown). This effect must be attributed to the favourable interaction between the MMT and the polymeric matrix since both the nanocomposites and the homopolymer were prepared using identical experimental conditions. However, the electrochemical stability (electrostability) of the PEDOT–MMT nanocomposites is lower than that of PEDOT homopolymer. This feature is illustrated in Fig. 4, which shows the control voltammograms from −0.50 V to 1.60 V for 30 consecutive oxidation–reduction cycles of PEDOT and PEDOT–MMT (5% w/w) films. Thus, the incorporation of MMT makes more difficult the access and escape of the dopant ions along the oxidation and reduction processes, respectively. Table 1 compares the performance of the nanocomposites with that of PEDOT homopolymer in terms of electroactivity and electrostability. Specifically, for PEDOT–MMT the cathodic and anodic areas recorded along the 30th cycle indicated a loss of electrostability and electroactivity ranging from 22% to 38% and from 7% to 18%, respectively, while for PEDOT homopolymer the loss of electrostability and electroactivity after 30 cycles were 25% and 3%, respectively.

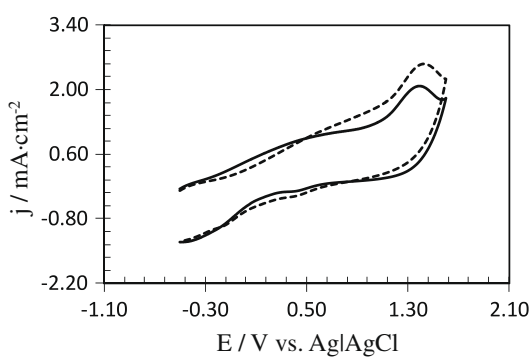

Fig. 3. Control voltammograms for the oxidation of PEDOT homopolymer (solid curve) and PEDOT–MMT (5% w/w) (dashed curve) films on 4 cm^2 steel electrode in distilled water with 0.1 M $LiClO_4$, at 100 mV·s^{-1} and 25 °C. Initial and final potentials: −0.50 V; reversal potential: 1.60 V.

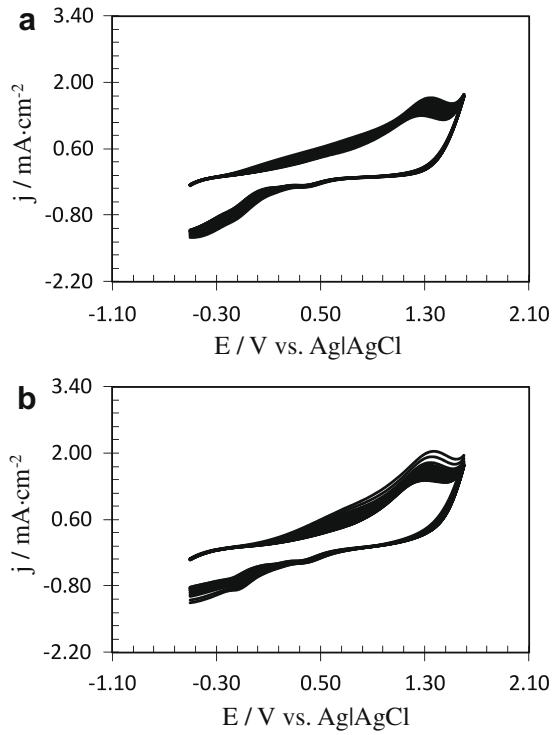

Fig. 4. Control voltammograms for 30 consecutive oxidation–reduction cycles of PEDOT (a) and PEDOT–MMT (5% w/w) (b). The conditions used to record the voltammograms were identical to those described in Fig. 3.

3.2. Distribution of the MMT in the nanocomposites

Transmission electron microscopy (TEM) was used to visualize the exfoliation of the clay in PEDOT–MMT nanocomposites. Thus, preparation of the TEM samples by ultramicrotome allows to cut the nanocomposites perpendicularly to the electrode surfaces and, therefore, to image the distribution of the clay within the polymeric matrix (intercalated or exfoliated). TEM micrographs of PEDOT–MMT nanocomposites reveal that, independently of the clay concentration, MMT is exfoliated into individual platelets within the polymeric matrix. This is illustrated in Fig. 5 for the PEDOT–MMT (5% w/w) and PEDOT–MMT (10% w/w) nanocomposites. These results confirm that the strategy used to prepare PEDOT–MMT nanocomposites successfully retains the exfoliated structure of the clay.

XRD patterns provide helpful information about the *d*-spacing of the MMT, the homopolymer and the nanocomposites by following Bragg's law at peak positions. It can be seen from Fig. 6 that the XRD pattern of the MMT is clearly different from those of the nanocomposites at low angles. Strong diffraction peaks at $2\theta = 7.04°$ (d_{100}) and $2\theta = 19.80°$ are displayed for the MMT. These reflections are extinguished in the diffractograms of the nanocomposites (data not shown for nanocomposites with 1% and 10% w/w of

Table 1
Loss of electroactivity and electrostability after 30 consecutive oxidation–reduction cycles for PEDOT homopolymer and PEDOT–MMT nanocomposites.

# Material	Loss of electroactivity (%)	Loss of electrostability (%)
PEDOT	25	3
PEDOT–MMT (1% w/w)	7	22
PEDOT–MMT (5% w/w)	11	34
PEDOT–MMT (10% w/w)	18	38

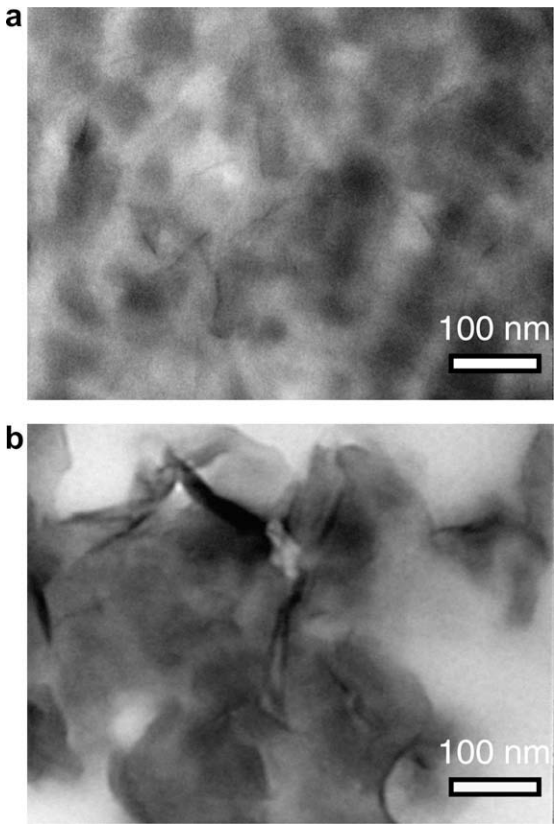

Fig. 5. TEM micrographs of (a) PEDOT–MMT (5% w/w) and (b) PEDOT–MMT (10% w/w).

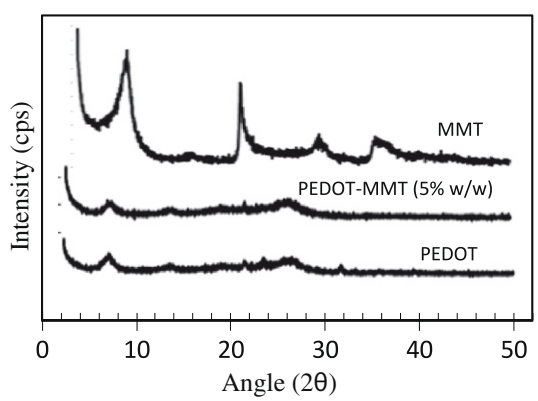

Fig. 6. XRD patterns of MMT, PEDOT and PEDOT–MMT (5% w/w).

MMT). Moreover, the broad peak detected in PEDOT–MMT diffractograms at $2\theta = 6.52°$ was also found in the pattern of PEDOT homopolymer (Fig. 6). These features confirm the exfoliation of the MMT layers in the polymer matrix of the nanocomposites supporting the images obtained by TEM.

3.3. Electrical conductivity

The σ_0 values measured for the three PEDOT–MMT nanocomposites and the PEDOT homopolymer are displayed in Table 2. It is worth noting that the σ_0 obtained in this work for perchlorate-doped PEDOT is similar to that previously reported for the polystyrene sulfonate-doped homopolymer, i.e. 1–2 $S{\cdot}cm^{-1}$ [47]. On the other hand, inspection of the σ_0 values determined for the PEDOT–MMT nanocomposites indicates that the incorporation of the clay does not produce significant changes with respect to the homopolymer, being in all cases of the same order of magnitude. Thus, although MMT typically acts as an inhibitor because it is not electronically conductive material, the exfoliated distribution achieved in this work minimizes this effect. Interestingly, the σ_0 values listed in Table 2 for PEDOT–MMT nanocomposites are significantly higher than those recently reported for exfoliated PEDOT–MMT nanocomposites doped with polystyrene sulfonate, i.e. σ_0 ranged from $5{\cdot}10^{-7}$ to $8{\cdot}10^{-2}$ $S{\cdot}cm^{-1}$ depending on the modifications introduced in the clay to facilitate the exfoliation [31].

Fig. 7 represents the temporal evolution of σ_0 for PEDOT homopolymer and PEDOT–MMT (5% w/w). As can be seen, the incorporation of the clay produces a drastic reduction of the electrical stability. Thus, the σ_0 of PEDOT–MMT (5% w/w) becomes practically negligible after 17 days, while that of the homopolymer decreased from 5.6 to 1.4 $S{\cdot}cm^{-1}$ after 35 days. The behaviour showed by PEDOT–MMT (1% w/w) and PEDOT–MMT (10% w/w) indicates that the loss of electrical stability increases with the concentration of clay.

3.4. Morphology

The average thickness determined for PEDOT and PEDOT–MMT is included in Table 2. As it was expected, the thickness of the film increases with the concentration of MMT. The morphological analysis has been focused on PEDOT and PEDOT–MMT (5% w/w), the latter being considered as the most representative nanocomposite. Fig. 8a shows an AFM image of the surface of PEDOT homopolymer, which

Table 2
Electrical conductivity (σ_0), average thickness (ℓ) and average RMS roughness (r) of PEDOT homopolymer and PEDOT–MMT nanocomposites. In all cases films were generated on a steel substrate by chronoamperometry using a constant potential of 1.10 V and a polymerization time $\theta = 300$ s.

#	σ_0 ($S{\cdot}cm^{1}$)	ℓ (μm)	r (nm)
PEDOT	5.5	0.84	153
PEDOT–MMT (1% w/w)	3.8	0.92	–
PEDOT–MMT (5% w/w)	2.7	1.02	112
PEDOT–MMT (10% w/w)	1.3	1.26	–

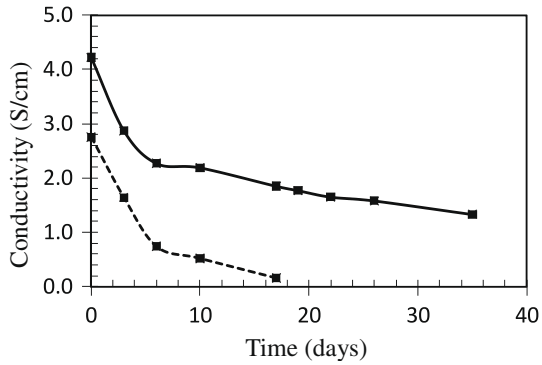

Fig. 7. Temporal evolution of the electrical conductivity (σ_0, in S·cm^{-1}) for the PEDOT homopolymer (solid line) and PEDOT–MMT (5% w/w) nanocomposite (dashed line).

exhibits an irregular, agglomerated and heterogeneous surface. However, the incorporation of MMT (5% w/w) produces a drastic change in this morphology, which is illustrated by the AFM image showed in Fig. 8b. Thus, the surface becomes more homogeneous, the irregularities produced by agglomerations being less sharp. This flatten effect, which is also evidenced by a significant reduction of the RMS roughness (Table 2), i.e. r decreases from 153 nm to 112 nm upon the incorporation of MMT (5% w/w), has been previously described for other heterocyclic conducting polymers, e.g. polypyrrole [48]. Thus, it was proposed that the presence of the clay in the polymerization medium reduces the molecular weight of the polymer [48].

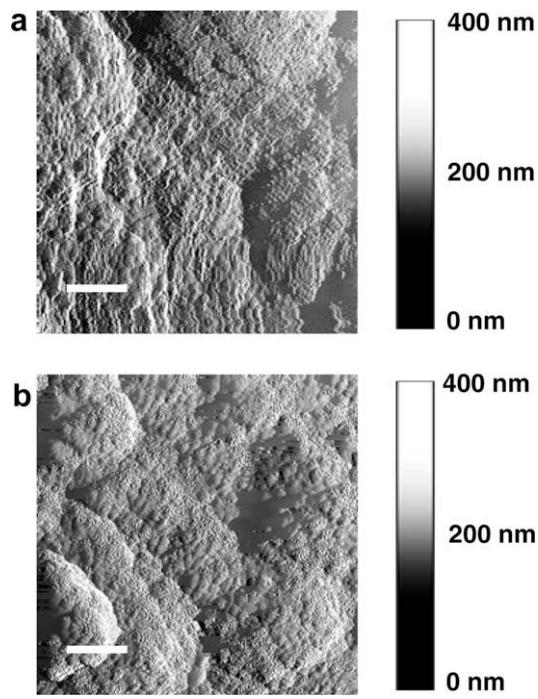

Fig. 8. AFM images of PEDOT homopolymer (a) and PEDOT–MMT (5% w/w) (b) films. Scale bar: 1 μm.

4. Conclusions

PEDOT–MMT nanocomposites have been prepared by anodic electropolymerization under a constant potential of 1.10 V into a $LiClO_4$ aqueous solution. Structural characterization using TEM and XRD indicates that the clay is exfoliated in the PEDOT matrix, which represents a significant improvement with respect to the intercalative structure usually found in conducting polymer–clay nanocomposites. Interestingly, the electroactivity of PEDOT–MMT nanocomposites, which increases with the concentration of clay, is higher than that of individual PEDOT, whereas the electrostability is only slightly lower for the former than for the latter. These results indicate that PEDOT–MMT nanocomposites are potential candidates for the fabrication of devices able to store charge. Additionally, the electrical conductivities of the nanocomposites and the homopolymer are very similar. However, the clay reduces significantly the electrical stability of the conducting polymer. The overall of the results evidences that anodic electropolymerization is a suitable procedure for the fabrication of exfoliated conducting PEDOT–clay nanocomposites with reliable properties. The materials reported in this work represent a significant improvement with respect to PEDOT–MMT, PAni–MMT and PPy–MMT prepared without previous modification of the clay. These nanocomposites usually present intercalative structures, the only advantage induced by the clay being, in general, the improvement of the thermal stability. Moreover, it should be emphasized that the introduction of special chemical modifications in the MMT, which is usually complicated and expensive, is not required to succeed with the strategy reported in this work.

Acknowledgements

This work has been supported by MICINN and FEDER funds (Project Nos. MAT2009-09138 and MAT2009-11503), by the International Cooperation Program from Brazilian and Spanish Education Ministries CAPES-MICINN (PHB2007-0038-PC), and by the DIUE of the Generalitat de Catalunya (Contract Nos. 2009SGR925 and 2009SGR1208). Support for the research of C.A. was received through the prize "ICREA Academia" for excellence in research funded by the Generalitat de Catalunya. D.A. thanks financial support through a FPU-UPC grant.

References

[1] Hasegawa N, Okamoto H, Kawasumi M, Kato M, Tsukigase A, Usuki A. Macromol Mater Eng 2000;180–181:76.
[2] Alexandre M, Dubois P. Mater Sci Eng 2000;28:1.
[3] Gilman JW, Jackson CL, Morgan AB, Hayyis Jr R, Manias E, Giannelis EP, et al. Chem Mater 2000;12:1866.
[4] Biswas M, Ray SS. Adv Polym Sci 2001;155:167.
[5] Zheng QH, Yu AB, Lu GQ, Paul DRJ. Nanosci Nanotech 2005;5:1574.
[6] Chen B, Evans JRG. Polymer 2008;49:5113.
[7] Paul DR, Robeson LM. Polymer 2008;49:3187.
[8] Skotheim TA, Reynolds JR, editors. Handbook of conducting polymers, 3rd ed. Boca Raton: CRC Press; 2007.
[9] Singhal R, Datta M. J Appl Polym Sci 2007;103:3299.
[10] Yoshimoto S, Ohashi F, Kameyama T. Macromol Rapid Commun 2004;25:1607.
[11] Kim BH, Jung JH, Hong SH, Kim JW, Choi HJ, Joo J. Curr Appl Phys 2001;1:112.

[12] Soundararajah QY, Karunaratne BSB, Rajapakse RMG. Macromol Chem Phys 2009;113:850.
[13] Yoshimoto S, Ohashi F, Ohnishi Y, Nonami T. Synth Metals 2004;145:265.
[14] Kim BH, Jung JH, Kim JW, Choi HJ, Joo J. Synth Metals 2001;117:115.
[15] Aranda P, Darder M, Fernández-Saavedra R, López-Blanco M, Ruiz-Hitzky E. Thin Solid Films 2006;495:104.
[16] Yeh J-M, Chin C-P, Chang S. J Appl Polym Sci 2003;88:3264.
[17] Hm HongS, Kim BH, Joo J, Kim JW, Choi HJ. Curr Appl Phys 2001;1:447.
[18] Kassim A, Mahmud HNME, Adzmi F. Mater Sci Semiconduc Proc 2007;10:246.
[19] Boukerma K, Piquemal J-Y, Chehimi MM, Mravcakova M, Omastova M, Beaunier P. Polymer 2006;47:569.
[20] Kim JW, Lui F, Choi HJ, Hong SH, Joo J. Polymer 2003;44:289.
[21] Pei Q, Zuccarello G, Ahlskog M, Inganas O. Polymer 1994;35:1347.
[22] Groenendaal L, Jonas G, Freitag D, Pielartzik H, Reynolds JR. Adv Mater 2000;12:481.
[23] Alemán C, Teixeira-Dias B, Zanuy D, Estrany F, Armelin E, del Valle LJ. Polymer 2009;50:1965.
[24] Estrany F, Aradilla D, Oliver R, Armelin E, Alemán C. Eur Polym J 2008;44:1323.
[25] Estrany F, Aradilla D, Oliver R, Alemán C. Eur Polym J 2007;43:1876.
[26] Armelin E, Menezguzzi A, Ferreira CA, Alemán C. Surf Coat Technol 2009;2003:3763.
[27] Murugan VA, Kwon C-W, Campet G, Kale BB, Maddanimah T, Vijayamohanan K. J Power Sources 2002;105:1.
[28] Murugan VA, Viswanath AK, Campet G, Gopinath CS, Vijayamohanan K. Appl Phys Lett 2005;87:243511.
[29] Han Y, Lu Y. Synth Met 2008;158:744.
[30] Leta S, Aranda P, Fernández-Saavedra Margeson R, Detelliera C, Ruiz-Hitzky E. J Mater Chem 2008;18:2227.
[31] Han Y, Lu Y. J Appl Polym Sci 2009;111:2400.
[32] do Nascimento GM, Constantino VR, Landers R, Temperini MLA. Macromolecules 2004;37:9373.
[33] Goddard YA, Vold RL, Hoatson GL. Macromolecules 2003;36:11662.
[34] Zeng QH, Wang DZ, Yu AB, Lu GQ. Nanotechnology 2002;13:549.
[35] Hoang HV, Holze R. Chem Mater 2006;18:1976.
[36] Leta S, Aranda P, Ruiz-Hitzky ER. Appl Clay Sci 2005;28:123.
[37] Yoshimoto S, Ohasi F, Kameyama T. Macromol Rapid Commun 2005;26:461.
[38] Mravcakova M, Boukerma K, Omastova M, Chehimi MM. Mater Sci Eng 2006;26:306.
[39] Jui MY, Shir JL, Chiung YL, Pei CW. Chem Mater 2001;13:1131.
[40] Bae WJ, Kim KH, Jo WH, Park YH. Polymer 2005;46:10085.
[41] Castagno KRL, Dalmoro V, Mauler R, Azambuja D. J Polym Res, in press. doi:10.1007/s10965-009-9353-0.
[42] Murugan AV, Gopinath CS, Vijayamohanan K. Electrochem Commun 2005;7:213.
[43] Liu YC, Tsai CJ. Chem Mater 2003;15:320.
[44] Ocampo C, Oliver R, Armelin E, Alemán C, Estrany F. J Polym Res 2006;13:193.
[45] Schirmeisen M, Beck F. J Appl Electrochem 1989;19:401.
[46] Brillas E, Carrasco J, Oliver R, Estrany F, Vilar J, Morlans JM. Electrochim Acta 2000;45:4049.
[47] Timparano S, Kemerink M, Touwslager FJ, De Kok MM, Schrader S. Chem Phys Lett 2004;394:339.
[48] Yeh JM, Chin CP, Chang S. J Appl Polym Sci 2003;88:3264.